ChemPubSoc Europe

DOI: 10.1002/open.201700052

Open Access ChemistryOPEN Full Papers

Dispersion Interactions and the Stability of Amine Dimers

Robin Guttmann and Alexander F. Sax*[a]

Weak, intermolecular interactions in amine dimers were studied by using the combination of a dispersionless density functional and a function that describes the dispersion contribution to the interaction energy. The validity of this method was shown by comparison of structural and energetic properties with data obtained with a conventional density functional and the coupled cluster method. The stability of amine dimers was shown to depend on the size, the shape, and the relative orientation of the alkyl substituents, and it was shown that the stabilization energy for large substituents is dominated by dispersion interactions. In contrast to traditional chemical explanations that attribute stability and condensed matter properties solely to hydrogen bonding and, thus, to the properties of the atoms forming the hydrogen bridge, we show that without dispersion interactions not even the stability and structure of the ammonia dimer can be correctly described. The stability of amine dimers depends crucially on the interaction between the non-polar alkyl groups, which is dominated by dispersion interactions. This interaction is also responsible for the energetic part of the free energy interaction used to describe hydrophobic interactions in liquid alkanes. The entropic part has its origin in the high degeneracy of the interaction energy for complexes of alkane molecules, which exist in a great variety of conformers, having their origin in internal rotations of the alkane chains.

1. Introduction

Although it has been known for a rather long time that a large part of the stabilization energy of molecular complexes is due to dispersion interactions,[1–5] the structure and stabilization of large biological systems are frequently attributed to hydrogen bonding only.[6–12] Traditionally, hydrogen bonding is considered as the stabilization of complexes owing to the occurrence of a characteristic atom group A–H···B connecting a proton donor molecule R1–A–H to a proton acceptor molecule B–R2; R1 and R2 are substituents and A and B are atoms more electronegative than hydrogen. A–H is a polar covalent bond in the donor molecule and B is a Lewis base in the acceptor molecule. That dispersion interactions are also important for the structure of molecular complexes has been stressed only recently.[13] Also, hydrophobic interactions, which are considered to be crucial for the understanding of protein folding, are dominated by dispersion interactions.[14] Bonding means stabilization of molecular systems, it is measured by the binding energy; if the result of bonding is called a bond, then one can say that the binding energy is a measure of the bond strength. For most chemists, bonds are also connected to atom groups with geometric properties such as distances and angles, properties that the central moiety A–H···B in a hydrogen-bonded complex has. In this sense, it makes sense to say that a hydrogen bond (HB) stabilizes the complex. Some chemists prefer to speak of a hydrogen bridge instead of a hydrogen bond, thus stressing structural aspects instead of aspects of stability. When we say a structure has one HB, we always claim the presence of one connecting A–H···B group.

The concept of hydrophobic interactions was introduced by Kauzmann[15] in 1959 to explain protein folding by the analogy with the transfer of a non-polar solute from water into a non-polar solvent. According to Kauzmann, the transfer is due to the poor solubility of the solute in water. Kauzmann used originally the term "hydrophobic bond", which was later replaced by "hydrophobic interaction" because there are no atom groups that can be made responsible for the bonding interaction.[16] Wolfenden and Lewis[17] explained the poor solubility of hydrocarbons in water by assuming "that a strong favorable interaction among alkane molecules in liquid alkanes gives a strong favorable transfer energy for passage of an alkane from vapor into liquid alkane."[14] The term hydrophobic interactions is thus used with two different meanings, first to describe the removal of a non-polar surface from contact with water, that is, a repulsive interaction; a second meaning is the direct attractive interaction between non-polar aliphatic groups, explaining, for example, the good solubility of alkane molecules in liquid alkane mentioned by Wolfenden and Lewis.[17] Both processes involve condensed matter phases and this demands use of free energy. Whereas the energy contribution to the free energy is caused by the basic intermolecular interactions, the explanation of the entropy contribution at the molecular level requires knowledge of the cardinality of the set

[a] R. Guttmann, Prof. Dr. A. F. Sax
Department of Chemistry, University of Graz
Heinrichstrasse 28, 8010 Graz (Austria)
E-mail: alexander.sax@uni-graz.at

Supporting Information and the ORCID identification number(s) for the author(s) of this article can be found under https://doi.org/10.1002/open.201700052.

of energetically equivalent structures of interacting molecules, because the entropy of a system state is directly proportional to the logarithm of the state's degeneracy. We shall show that systems with interacting alkyl chains have a large number of equilibrium structures with similar energies and this quasi-degeneracy contributes to the entropic part of the free energy.

Weak, intermolecular interactions, also called non-covalent interactions,[18,19] are the origin of hydrogen bonding and hydrophobic interactions with the second meaning. The stabilization energy for weakly bonded molecular systems is at least one order of magnitude smaller than that of bond energies in covalent bonds. All non-covalent interactions are caused by the four basic interactions: 1) electrostatics, that is, the interaction between static multipoles; 2) induction, that is, the interaction between static multipoles in one molecule and induced multipoles in a second molecule; 3) dispersion; and 4) exchange repulsion, that is, a repulsion between electrons owing to their indistinguishability. The interaction between static multipoles may be attractive or repulsive, depending on the relative orientation of the interacting molecules. Induction can be interpreted as the classical interaction of static multipole moments in one molecule with multipoles induced in the polarizable electron density of the second molecule. Induction is always attractive, it depends on the static polarizability of the molecule in which the multipole is induced. Dispersion interaction is due to the correlation of the electron motions in one molecule with those of the electrons in the other molecule and is thus of purely quantum origin. The fluctuations in the electron density of one molecule, mainly caused by the non-deterministic electron motions, give rise to multipole moments, which induce multipole moments in the other molecule such that the interaction between them stabilizes the molecular system. There are, however, many more possible explanations of what causes the charge fluctuations or interpretations of the dispersion interaction, see, for example, the book by Salam.[20] Like induction, dispersion is always attractive; its strength depends on the dynamic polarizabilities of the interacting molecules. It is a ubiquitous interaction between systems of electrons in motion and occurs also in completely non-polar systems such as noble gas atoms. Nevertheless, electrostatics is frequently considered to be the most important attractive interaction in hydrogen-bonded systems. Finally, exchange repulsion is a ubiquitous destabilizing interaction between indistinguishable Fermions. The amount each interaction contributes to a non-covalent interactions determines its character.

The range of the four basic interactions is very different. Exchange repulsion decreases exponentially with the distance, it has the shortest range of all basic interactions. The interaction between permanent multipoles (2^l) and (2^L), such as monopoles ($l=0$), dipoles ($l=1$), quadrupoles ($l=2$) goes as $r^{-(l+L+1)}$ with the distance r between the multipoles; the range of the interaction between permanent 2^l-poles and induced 2^L-poles is much smaller than that between permanent multipoles, it goes as $r^{-2(l+L+1)}$, the same relation holds for the multipoles in dispersion interactions. For uncharged molecules, the interaction between dipoles has the longest range, this is true for permanent and for induced dipoles. Except for monopole–monopole interactions, which are indeed isotropic, all interactions between higher multipoles are genuinely anisotropic; the lowest anisotropy is found for dispersion interactions, which are therefore frequently regarded as being approximately isotropic.

Long-range or London dispersion interactions caused by the correlation of fluctuating dipoles are operative even at distances where the overlap between the wave functions of the interacting molecules is close to zero. In this case, it is not necessary to antisymmetrize the product of the wave functions of the interacting molecules when perturbation theory is used to calculate the interaction contributions. Many so-called empirical dispersion corrections schemes have been proposed for calculating long-range dispersion contributions without quantum theoretical methods. See, for example, reviews by Grimme and co-workers.[21,22] When the interacting molecules are so close that speaking of weakly interacting molecules becomes meaningless, electron correlation must be accounted for by proper wave functions or by using density functionals (DF) for the whole molecular system. Both types of electron correlation should merge seamlessly in the region of medium-range correlation where antisymmetrization of the wave functions of the interacting molecules is mandatory and interactions between higher multipoles must be accounted for. Semilocal or hybrid Kohn–Sham DFs cannot describe long-range electronic correlation effects, and thus no London dispersion interactions, but it is not clear whether they cover a certain amount of medium- or short-range dispersion interaction. It is, however, possible to develop powerful dispersion correction methods to remedy this shortcoming.[21,22]

Although all three attractive interactions contribute to non-covalent interactions, there are chemists who claim that hydrogen bonding is purely electrostatic; some scientists consider only interactions in the central moiety, as if interaction between the central moiety and the substituents did not exist. In a recent study of hydrogen bonding in alcohol dimers,[23] we showed that indeed all four interactions contribute to hydrogen bonding and that it is misleading to discuss only the contribution of the central moieties A–H···B to the stabilization of hydrogen-bonded systems, because they are only the connecting part in the molecular system R1–A–H···B–R2; with increasing size of the substituents the interactions between them increase as well and eventually may become dominant. For large substituents dispersion interactions dominate.

In this study, we investigate the stabilization of primary amines in dimers. According to Jeffrey's classification,[9] hydrogen bonds in amine dimers are classified as moderate, as are the hydrogen bonds in alcohol dimers; nevertheless, the stabilization energies in amine dimers are markedly smaller than those in alcohol dimers. Traditionally, such differences have been explained by the different electronegativities of nitrogen and oxygen, resulting in smaller bond dipole moments in N–H bonds than in the O–H bonds. This is an example of an explanation reducing hydrogen bonding to electrostatic interactions in the central moiety only. In this study, we show that without dispersion interactions neither the structure nor stability of

amine dimers can be correctly described, a result we found also for alcohol dimers.[23] We find that the size and relative position of the substituents is crucial for the dimer stabilization, and that dimers with very large substituents become unstable if dispersion is neglected. Furthermore, we find especially for amines with large, parallel aligned substituents several dimer structures with similar energy, which is due to the large number of conformational isomers resulting from internal rotations about carbon–carbon single bonds. The number of energetically equivalent structures will increase if more than two alkyl chains are parallel aligned, as is the case in condensed matter systems like liquids or solids.

2. Methods

In this paper, we will use the term interaction energy for all interaction components especially for their representations by graphs; stabilization energy always means the difference between the energies of the dissociated dimer and it equilibrium geometry; we abstain from using the term hydrogen-bond energy. When we say in this paper that an interaction energy is smaller than another, we speak about the absolute values.

System stabilization is a process related to changes of the system geometry. To get the distance dependence of the interaction energy without intramolecular energy contributions from relaxation of the interacting molecules, we study the energy curves for rigid dissociation of the dimer. To do this, we optimized the equilibrium geometries of the dimers and then separated the monomers without allowing geometry relaxation.

The dispersionless DF, dIDF,[24] was designed to reproduce for interacting systems the dispersionless interaction energy defined as the difference of coupled-cluster interaction energies and the dispersion contributions to the interaction energy calculated with SAPT(DFT) (symmetry-adapted perturbation theory based on density functional theory).[25,26] The dispersion contribution to the total interaction energy, D_{as}, is calculated as the sum of contributions from atom pairs, where each of the two interacting molecules contributes one atom (intermolecular atom pairs).[27] The parameters describing the atomic contributions were fitted against the SAPT(DFT) energies. The sum of dIDF and D_{as} is denoted as dIDF + D_{as}. Whether conventional Kohn–Sham or hybrid DFs cover a certain amount of dispersion energy cannot be answered with certainty. Interaction energies calculated in a supermolecular approach by using such methods may yield a very good agreement with results from high-quality methods, but this agreement could be fortuitous. Manifest shortcomings of such DFs can be cured with empirical correction schemes. For several systems, we compared dIDF + D_{as} results with those obtained with B3LYP[28] and Grimme's D2 and D3 dispersion correction,[29,30] these methods are labeled B3LYP + D2 and B3LYP + D3, respectively. Both D_{as} and Grimme's D2 and D3 corrections are basis set independent. For some structures of the cyclic ammonia dimer and the methylamine dimer, taken from the BEGDB data base,[31] we compared DFT energies with CCSD(T) energies obtained at the complete basis set limit (CBS).

For the basis set studies, we used Dunning's unaugmented basis sets cc-pVXZ and the augmented basis sets aug-cc-pVXZ (X = D,T,Q, and 5);[32–35] we use in this paper XZ (X = D,T,Q, and 5) as a shorthand notation for the unaugmented and aXZ for the corresponding augmented basis sets. Geometry optimization of amine dimers was performed with the DZ basis set. The usual method/basis notation is used throughout in this paper. All interaction energies and gradients were corrected for the basis set superposition error by using the counterpoise correction method by Boys and Bernardi.[36]

The DFT calculations were performed with NWChem 6.2,[37] gradients for dIDF + D_{as} were implemented in a local copy of this program system.

Start geometries were created with Avogadro.[38]

3. Investigated Systems

In this study, we investigate the parent ammonia dimer $(NH_3)_2$ and the homomolecular dimers of primary amines with the following linear and branched alkyl groups: methyl (Me), ethyl (Et), *n*-propyl (*n*Pr), *n*-butyl (*n*Bu), *iso*-propyl (*i*Pr), and *tert*-butyl (*t*Bu). This allows us to study the influence of shape and size of the substituents on the dimer properties. In the following, amine dimers are denoted just by the name of the alkyl group, for example, Me_2 instead of $(MeNH_2)_2$, etc.

For the ammonia dimer several structures exist, but we investigated only two C_s structures with a single HB, denoted staggered and eclipsed, and a cyclic one with two HBs (see Figure 1). The eclipsed structure corresponds always to a local

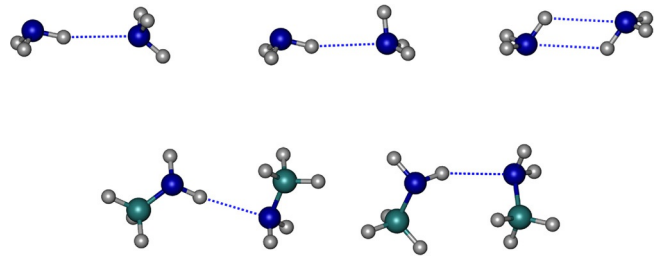

Figure 1. First row: Equilibrium structures of staggered (left), eclipsed (middle), cyclic (right) $(NH_3)_2$. Second row: Equilibrium geometries of *cis*-Me_2 (left) and *trans*-Me_2 (right).

minimum on the potential energy surface and the staggered structure corresponds, basis set dependent, to either a local minimum or to a saddle point; therefore, we used only the eclipsed structure for comparison of cyclic and non-cyclic ammonia dimers and for the construction of the amine dimers. All amine dimers are connected by a single HB; the structures with linear alkyl groups (see Figure 2) were obtained in the following way. Starting from the eclipsed ammonia dimer, the most distant hydrogen atoms were substituted by methyl groups followed by unconstrained geometry optimization by using dIDF + D_{as}. Then, the most distant hydrogen atoms were replaced by methyl groups and the structure optimized, and so on. This gave a group of dimers with the most distant terminal methyl groups, called the *trans* group. The created alkyl

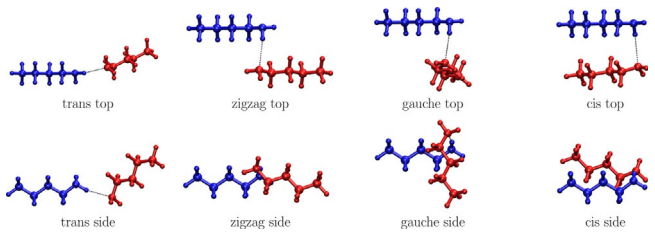

Figure 2. Top and side views of the four nBu$_2$ isomers.

groups are in an all-antiperiplanar conformation. This is also the way we constructed the alcohol dimers in our SAPT(DFT) study.[23] By using a different start geometry, we found another group of structures, called *zigzag*, which differ from the *trans* structures mainly by the angular structure of the central moiety.

When in the methyl groups of the dimethylamine dimer Me$_2$ the hydrogen atoms that are closest together are replaced by methyl groups, one gets the *cis* group of dimers; roughly speaking, the substituents are aligned parallel. In dimers with large substituents, two different alignments of the alkyl chains are possible, which we call *syn* and *anti* (see Figure 3). We also investigated a small number of structures where the alkyl groups are partially in clinal conformations. Discussion of *cis* dimers is always based on the *anti* structures.

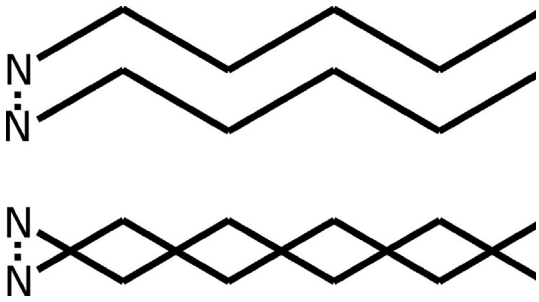

Figure 3. *Syn* (top) and *anti* (bottom) arrangement of the alkyl chains in *cis* dimers. The alkyl groups are in the all-antiperiplanar conformation.

Zigzag structures correspond to local minima only at the dlDF+D$_{as}$ level; optimization with B3LYP+D2 and B3LYP+D3 leads immediately to the more stable *gauche* structures, which are, somehow, in between the most stable *cis* and the unstable *zigzag* structures. For the small dimer Me$_2$, there is no difference between *cis* and *gauche*.

The fourth group consists of the amines with branched substituents; this group can be considered as being derived from Me$_2$ by successively replacing the methyl hydrogen atoms by methyl groups. Structures derived from the parent *trans*-Me$_2$ are labeled I, those derived from *cis*-MeNH$_2$ are labeled II.

4. Comparison of Methods

In the first part of this paper, we validate the dlDF+D$_{as}$ method. First, we study the basis set dependence of the three methods, dlDF+D$_{as}$, B3LYP+D2, and B3LYP+D3, and the influence of the dispersion energy or dispersion correction on the stabilization energies for the equilibrium structures of the non-cyclic and the cyclic ammonia dimers and *cis*-Me$_2$ and *trans*-Me$_2$. The equilibrium structures of the cyclic ammonia dimer[39] and of *cis*-Me$_2$[40] are taken from the BEGDB data base,[31] the eclipsed, non-cyclic ammonia dimer was optimized with the TZ basis, and *trans*-Me$_2$ was optimized with the DZ basis. Next, we compare the shapes of the potential curves for the rigid dissociation of the ammonia dimer and the methylamine dimer by using the three methods. Finally, we compare the equilibrium structures obtained by unconstrained optimization. For this comparison, we calculated equilibrium geometries of the two ammonia dimers and of all amine dimers.

4.1. Basis Sets

For the investigation of the basis set dependence we need only the dlDF and B3LYP energies given in Table 1. The energies including dispersion contributions are given in the Supporting Information. The stabilization energies shown in Figure 4 demonstrate, in addition, the influence of the dispersion contributions on the stabilization energies. We find for all systems and with both functionals: 1) convergence of the stabilization energies at the quintuple zeta level; and 2) that a5Z and 5Z values are essentially equal. We find that for the Me$_2$ dimers the a5Z values are larger by about 0.02 kJ mol^{-1} than the 5Z values, for the ammonia dimers the a5Z values are smaller than the 5Z values, by 0.01 kJ mol^{-1} for the non-cyclic and 0.07 kJ mol^{-1} for the cyclic dimer. We find uniform convergence behavior for the Me$_2$ dimers, but different convergence for the ammonia dimers, depending on the basis set type (augmented or unaugmented) and the dimer structure (cyclic or non-cyclic). For both Me$_2$ dimers, the stabilization energies are essentially converged at the TZ level with both augmented and unaugmented basis sets, frequently the TZ and the 5Z values are identical and the QZ values are slightly (0.01 kJ mol^{-1}) larger. This is found for both functionals. The maximum differences between the TZ, QZ, and 5Z values are not larger than 0.07 kJ mol^{-1} for both dimers, both DFs, and both types of basis sets.

The basis set convergence for the two ammonia dimers is very different for the two DFs. With dlDF and unaugmented

Table 1. Basis set dependence of $(NH_3)_2$ with 1 HB and 2 HB and Me$_2$ *trans* and *cis*.

	$(NH_3)_2$ 1 HB		$(NH_3)_2$ 2 HB		*trans*-Me$_2$		*cis*-Me$_2$	
Basis	dlDF	B3LYP	dlDF	B3LYP	dlDF	B3LYP	dlDF	B3LYP
DZ	−4.55	−9.68	−1.85	−8.43	−0.73	−8.40	+0.18	−8.59
TZ	−5.24	−9.61	−3.49	−9.57	−1.50	−8.62	−0.75	−8.99
QZ	−5.09	−9.45	−3.42	−9.42	−1.47	−8.62	−0.77	−9.01
Z	−5.07	−9.42	−3.30	−9.22	−1.45	−8.61	−0.75	−9.00
aDZ	−4.64	−9.13	−2.77	−8.79	−1.12	−8.32	−0.44	−8.76
aTZ	−5.10	−9.36	−3.28	−9.11	−1.49	−8.57	−0.74	−8.95
aQZ	−5.09	−9.41	−3.29	−9.17	−1.49	−8.62	−0.80	−9.02
a5Z	−5.06	−9.42	−3.24	−9.15	−1.48	−8.63	−0.77	−9.02

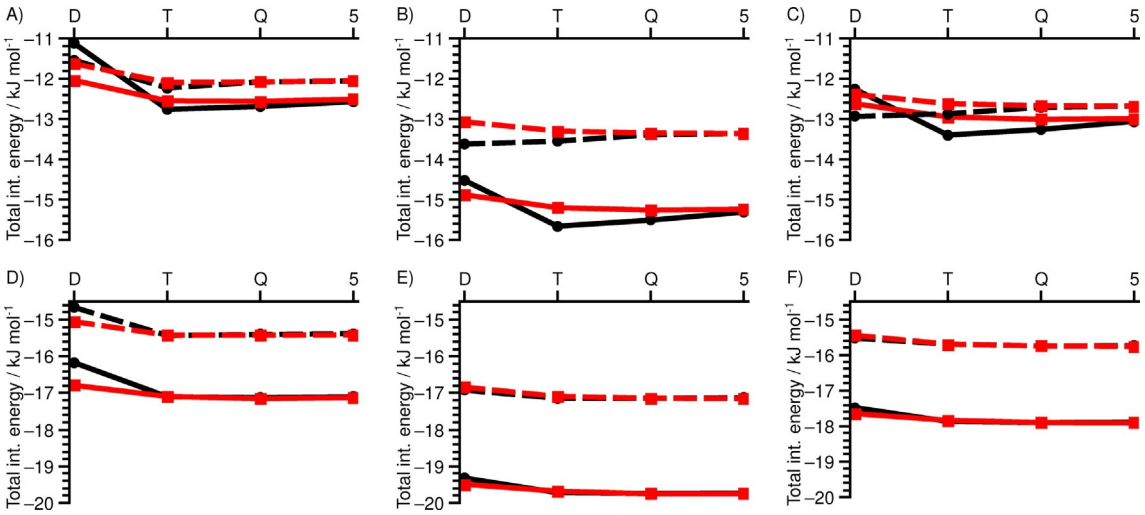

Figure 4. Basis set study of the stabilization energy (total interaction energy) with the density functional based methods dlDF (A) and (D), B3LYP + D2 (B) and (E) and B3LYP + D3 (C) and (F). A–C) Ammonia dimer with two different geometries, where the full line is the cyclic structure with two HBs from BEGDB and the dashed line corresponds to the noncyclic with one HB. D–F) Me_2 with *cis* (full lines), geometry from BEGDB, and *trans* geometry (dashed lines); augmented aXZ (red) and unaugmented XZ (black) basis sets from Dunning with X = D,T,Q,5 are used.

basis sets, we observe for both dimers a strong increase of the stabilization energy when going from DZ to TZ and then a monotonic decrease to 5Z, the maximum variation is for the non-cyclic dimer, which is roughly three times as large as for the cyclic dimer. With augmented basis sets, the variations are smaller and the aTZ values are essentially equal to the a5Z values. With B3LYP, we find for the cyclic dimer essentially the same convergence as with dlDF but for the non-cyclic dimer we find with unaugmented basis sets a monotonic decrease and with augmented basis sets a monotonic increase of the stabilization energies. As for the Me_2 dimers, the 5Z and a5Z energies are essentially equal, and the aTZ energies are very close to the a5Z values.

The different convergence of the counterpoise corrected stabilization energies shows the need for large basis sets for small systems like the ammonia dimers, whereas in the Me_2 dimers the additional basis sets from the methyl groups augment the basis and, therefore, the small unaugmented basis set TZ is sufficient to get reliable stabilization energies. TZ is therefore the basis of choice for calculating the stabilization energy in amine dimers. For the ammonia dimers, we need at least the aTZ basis set or the QZ basis set.

4.2. Dispersion Method

The differences between the basis set limits obtained for the three methods are caused by the different energies calculated with the DFs and the different contributions of dispersion interaction to the stabilization energy. This is what we find: for the non-cyclic ammonia dimer, the dispersion contributions are $-6.99\ kJ\,mol^{-1}$ (D_{as}), $-3.94\ kJ\,mol^{-1}$ (D2), and $-3.26\ kJ\,mol^{-1}$ (D3), for the cyclic dimer the respective values are $-9.27\ kJ\,mol^{-1}$, $-6.09\ kJ\,mol^{-1}$, and $-3.84\ kJ\,mol^{-1}$. When these dispersion contributions are added to the pure DFT a5Z energies, we get for the non-cyclic dimer stabilization energies of $-12.05\ kJ\,mol^{-1}$, $-13.36\ kJ\,mol^{-1}$, and $-12.68\ kJ\,mol^{-1}$ and for the cyclic dimer $-12.51\ kJ\,mol^{-1}$, $-15.24\ kJ\,mol^{-1}$, and $-12.99\ kJ\,mol^{-1}$, respectively. Comparison with the CCSD(T)/CBS value of $-13.14\ kJ\,mol^{-1}$ for the cyclic ammonia dimer shows that dlDF + D_{as} and B3LYP + D3 underestimate this value by −4.8% and −1.1%, whereas B3LYP + D2 overestimates it by 16.0%. By using these values, we find for the relative stabilities of the two dimers $-0.46\ kJ\,mol^{-1}$, $-1.88\ kJ\,mol^{-1}$, and $-0.31\ kJ\,mol^{-1}$, respectively. The smallest difference between the cyclic and the non-cyclic dimer is found with B3LYP + D3; the dlDF + D_{as} value is about 50% larger and the B3LYP + D2 is about six times larger.

The trend is similar for the Me_2 dimers. For *trans*-Me_2 the dispersion contributions are $-13.93\ kJ\,mol^{-1}$ (D_{as}), $-8.52\ kJ\,mol^{-1}$ (D2), and $-7.13\ kJ\,mol^{-1}$ (D3), and for *cis*-Me_2 they are $-16.35\ kJ\,mol^{-1}$, $-10.73\ kJ\,mol^{-1}$, and $-8.88\ kJ\,mol^{-1}$, respectively. As for the ammonia dimers, we find that the D_{as} values are about twice as large as the D3 corrections and that the D2 corrections are considerably larger than the D3 corrections. Adding the dispersion contributions to the pure a5Z energies gives the following stabilization energies: $-15.41\ kJ\,mol^{-1}$, $-17.15\ kJ\,mol^{-1}$, and $-15.76\ kJ\,mol^{-1}$, respectively, and $-17.12\ kJ\,mol^{-1}$, $-19.75\ kJ\,mol^{-1}$, and $-17.91\ kJ\,mol^{-1}$, for *cis*-Me_2, respectively. The dlDF + D_{as} energies are $0.35\ kJ\,mol^{-1}$ and $0.79\ kJ\,mol^{-1}$ smaller than the B3LYP + D3 energies. Comparison with the CCSD(T)/CBS value of $-17.36\ kJ\,mol^{-1}$ for *cis*-Me_2 shows that dlDF + D_{as} underestimates it by −1.4% and B3LYP + D3 overestimates it by +3.2%. We do not know, however, whether for larger dimers this trend continues and both DFT methods will overestimate the CCSD(T)/CBS values. The relative stabilities of the Me_2 dimers are $-1.71\ kJ\,mol^{-1}$, $-2.60\ kJ\,mol^{-1}$, and $-2.15\ kJ\,mol^{-1}$, respectively. These rather small energy differences are composed of differences in the DFT energies and the dispersion contributions. With dlDF, *cis*-Me_2 is by $0.71\ kJ\,mol^{-1}$ less stable than *trans*-Me_2, but the dif-

ference in the dispersion energy of $-2.42\ kJ\,mol^{-1}$ causes the higher stability of the *cis* dimer. With B3LYP, *cis*-Me_2 is more stable than *trans*-Me_2 by $0.39\ kJ\,mol^{-1}$ and with the D3 contribution *cis*-Me_2 is stabilized by an additional $1.75\ kJ\,mol^{-1}$.

4.3. Potential Energy Curves

The BEGDB data base contains information for the rigid dissociation of cyclic $(NH_3)_2$ and *cis*-Me_2. The potential energy curves are represented by the CCSD(T)/CBS interaction energies for supporting structures as functions of the monomer distances R, which is for $(NH_3)_2$ the $H\cdots N$ distance and for Me_2 it is the distance between the centers of mass of the two monomers. The monomer distances are given in reduced units, that is, ratios of the actual monomer distance and the equilibrium distance. For the dissociation of the amine dimer, five supporting structures with reduced distances R_{red} of 0.9, 1, 1.2, 1.5, and 2 are listed, and eight supporting structures with distance values of 0.9, 0.95, 1, 1.05, 1.1, 1.25, 1.5, and 2 for the dissociation of Me_2. We calculated for these structures the interaction energies with all DFT methods, for the ammonia dimer and for Me_2 we used the aTZ basis. The eight supporting structures for the Me_2 dissociation are sufficient to get smooth curves even for those methods having their minimum not at $R_{red}=1$; for the dissociation of the ammonia dimer, the five supporting structures give smooth curves for dlDF + D_{as} and B3LYP + D3, but for all other methods the five structures from the BEGDB data base are not sufficient, so we added three more supporting structures with R_{red} values of 0.95, 1.05, and 1.10.

Figure 5 shows the curves of the DFT interaction energies with and without dispersion contributions and the CCSD(T)/CBS reference curve. We see that the agreement of the dlDF + D_{as}, B3LYP + D3, and CCSD(T)/CBS curves is excellent, this is true not only for the position of the local minima and the depths of the potential well but also for the shape of the whole curves. With B3LYP + D2, the potential wells are too deep and the local minima are shifted to smaller values of the monomer distances.

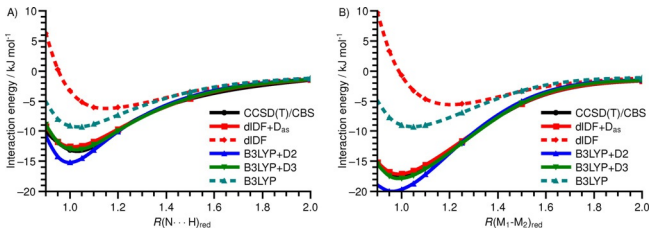

Figure 5. Potential curve (without relaxation of the monomer geometries) with the different methods with and without dispersion correction: A) $(NH_3)_2$, B) Me_2.

As the dlDF curves show, the sum of repulsive exchange and attractive electrostatics and induction can reproduce neither the equilibrium geometry nor the depth of the potential well as the local minima are shifted toward larger distances between the monomers and the depths of the local minima are only a fraction of the real stabilization energies. If the missing dispersion interaction is accounted for by adding D_{as} to dlDF, we get excellent agreement with the CCSD(T)/CBS curve.

In the B3LYP curves, the position of the local minima is shifted to smaller distances and the depth of the wells is increased. But only when the D3 correction is added to the B3LYP curves do the positions and the values at the local minima agree with the CCSD(T)/CBS results. It is tempting to assume that this is caused by a larger amount of short- or medium-ranged dispersion interaction covered by the B3LYP DF, but we resist this temptation for the reasons mentioned above. We might note, in passing, that we obtained similar results also for six other semilocal DFs (Guttmann, Sax, unpublished results), making this interpretation more plausible but still not logically correct.

The dlDF curves in Figure 5 also show that substitution of two hydrogen atoms in the ammonia dimer by methyl groups 1) increases the steepness of the repulsive branch of the dlDF energy curve, 2) decreases the depth of the potential well, and 3) shifts the position of the minimum to larger distances. From our SAPT study,[23] we know that with the increase of the number of atoms in the interacting monomers, all four interactions components increase in magnitude, but because the increase of exchange repulsion outweighs the increase of attractive electrostatics and induction, exchange is responsible for the destabilization of the dimer. It is the attractive dispersion contribution that shifts the minimum of the potential well back to smaller values and increases the well depth.

4.4. Equilibrium Geometries of Dimers

We know that the TZ basis is sufficient to get reliable stabilization energies for the Me_2 dimers but that the aTZ basis is necessary for the ammonia dimers. To check the influence of basis sets on the equilibrium geometries of the ammonia and the Me_2 dimers, we performed unconstrained geometry optimizations of these structures by using the DZ and TZ basis sets. For the Me_2 isomers, we find that DZ and TZ yield very similar geometry parameters (Guttmann, Sax, unpublished results).

For the ammonia dimers, we find a strong influence of the basis set and the start geometry on the equilibrium structures. With dlDF + D_{as} and DZ, the staggered structure is a local minimum but with TZ it is a saddle point; with B3LYP + D3 it is the other way around. This is the reason why we concentrate only on the eclipsed structure. With the DZ basis and a slightly deformed eclipsed starting geometry all methods found the eclipsed equilibrium structure; with the TZ basis, dlDF + D_{as} and B3LYP + D2 converged to the cyclic and only B3LYP + D3 converged to the eclipsed equilibrium structure. The cyclic structure was retained during a reoptimization with the smaller DZ basis. Only when the cyclic equilibrium structure obtained with dlDF + D_{as} was used as start geometry, did B3LYP + D3 with the TZ basis also find a cyclic equilibrium geometry. These findings suggest that the topography of the hypersurfaces for the ammonia dimer is dominated by several local minima of similar depth, which are not separated by large energy barriers and the stabilization energies, calculated with

Table 2. Total interaction energies (aTZ basis) for cyclic and non-cyclic $(NH_3)_2$ structures optimized with DZ and TZ.

	dlDF + D_{as}		B3LYP + D2		B3LYP + D3	
	DZ	TZ	DZ	TZ	DZ	TZ
non-cyclic	−12.09	–	−14.03	–	−13.31	−13.45
cyclic	−12.26	−12.38	−15.00	−15.28	–	−13.11

the aTZ basis (see Table 2), support this assumption. However, we did not check this assumption in detail.

For the geometry parameters, we find reasonable agreement between all three methods as Table S5 of the Supporting Information shows; dlDF + D_{as} yields shorter NH bonds than B3LYP, and a longer H···N distance; the N–N distance and the N-H-N bond angle are again very similar.

We calculated also for the eclipsed, non-cyclic equilibrium structures the stabilization energies with basis sets up to 5Z and found the same trends as for the cyclic ammonia dimer described above. The stabilization energies of non-cyclic structures are, as expected, slightly smaller than those of cyclic structures, all energies are given in Table S2 of the Supporting Information.

5. Structure and Stability of Amine Dimers

Geometry optimization of all amine dimers was done with the methods dlDF + D_{as} and B3LYP + D3 using basis set DZ. Stabilization energies were calculated only with dlDF + D_{as} and the TZ basis, for the discussion of the results we use only the dlDF + D_{as} data.

5.1. Optimized Structures

We calculated equilibrium structures of all *trans*, *cis*, and *gauche* amine dimers, as well as of amines with branched substituents. The great similarity of the equilibrium geometries obtained with dlDF + D_{as} and B3LYP + D3 are shown by overlays presented in Figures 6–10. The overlay was done with respect to the two nitrogen atoms and the two corresponding C_α atoms. All dimers are chiral molecules with the possibility of different signs for the dihedral angles C_α-N-N-C_α after geometry optimization. In the tables, all dihedral angles have positive signs. More geometry parameters can be found in the Supporting Informations (Tables S5–S7).

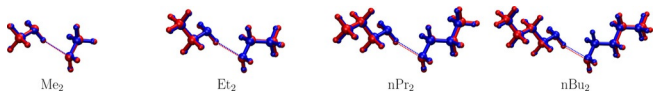

Figure 6. Overlay of *trans* structures obtained with dlDF + D_{as} (blue) and B3LYP + D3 (red).

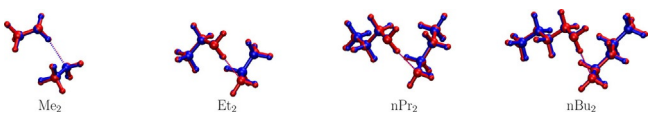

Figure 7. Overlay of *gauche* structures obtained with dlDF + D_{as} (blue) and B3LYP + D3 (red).

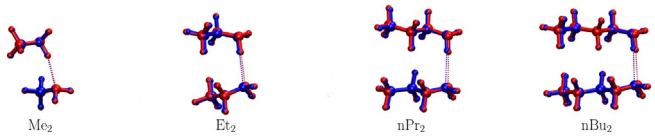

Figure 8. Overlay of *cis-anti* structures obtained with dlDF + D_{as} (blue) and B3LYP + D3 (red).

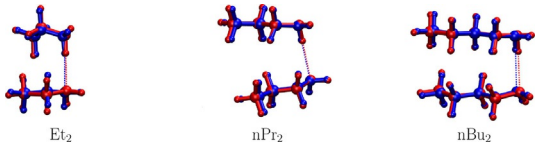

Figure 9. Overlay of *cis-syn* structures obtained with dlDF + D_{as} (blue) and B3LYP + D3 (red).

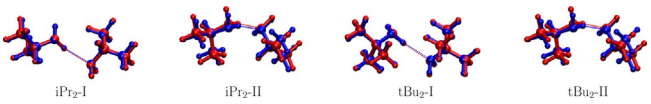

Figure 10. Overlay of branched structures obtained with dlDF + D_{as} (blue) and B3LYP + D3 (red).

There are no tremendous differences between the geometry parameters of the central moieties (see Tables 3 and 4). Whereas the N–H distance is in all dimers 0.98 Å, the H···N distance varies between 2.25 and 2.37 Å; short distances are found for *trans* and *gauche* structures, large values are found for the *cis* dimers with the largest substituents *n*Pr and *n*Bu. The N–N distance varies between 3.19 and 3.35 Å, again the largest distances are found in *cis* dimers with the largest substituents; the N-H···N angle varies between 161 and 176°, the smaller values are found in *trans* and *gauche* dimers, larger ones in *cis* dimers.

In *trans* dimers, the values of the C_α-N-N-C_α dihedral angle are rather uniform, but in *gauche* and *cis* dimers the value depends on the size of the substituents; with increasing size of the substituents the dihedral angles become similar. The distance between the terminal carbon atoms, C_ω–$C_{\omega'}$ can be used as a rough measure of the distance between the substituents. In *cis* dimers, this distance varies between 3.81 Å for Me_2 and 4.60 Å for *syn*-Pr_2; in *gauche* dimers, between 4.62 and 5.33 Å; for the branched dimers, this distance is not well defined and has no meaning. The smaller distances in the *cis* series are expected because the alkyl chains grow in parallel and attract each other; in the *gauche* series, an increase of alkyl chains is accompanied by a decrease of the distance between the terminal C atoms owing to the higher torsional flexibility of the substituents, together with large changes of the C_α-N-N-C_α dihedral angle. In the *trans* series, the distances between the terminal carbon atoms increase monotonically with increasing size of the substituents.

Table 3. Equilibrium geometry of dimers with non-branched substituents. Distances in Å, bond angles in degrees. τ is the C_α-N-N-C_α dihedral angle.

	trans				*gauche*				*cis-anti*			
System	N–N	H···N	N-H-N	τ	N–N	H···N	N-H-N	τ	N–N	H···N	N-H-N	τ
Me_2	3.21	2.25	164	176	3.19	2.26	161	71	3.20	2.26	161	71
Et_2	3.20	2.25	164	175	3.28	2.34	162	35	3.31	2.33	176	15
nPr_2	3.19	2.25	162	172	3.29	2.35	161	29	3.35	2.37	172	26
nBu_2	3.19	2.25	162	172	3.30	2.36	161	29	3.35	2.37	173	31

Table 4. Equilibrium geometry of dimers with branched substituents. Distances in Å, bond angles in degrees. τ is the C_α-N-N-C_α dihedral angle.

System	N–N	H···N	N-H-N	τ
iPr_2 I	3.20	2.25	164	180
iPr_2 II	3.21	2.25	166	−109
tBu_2 I	3.27	2.30	172	−135
tBu_2 II	3.31	2.35	166	80

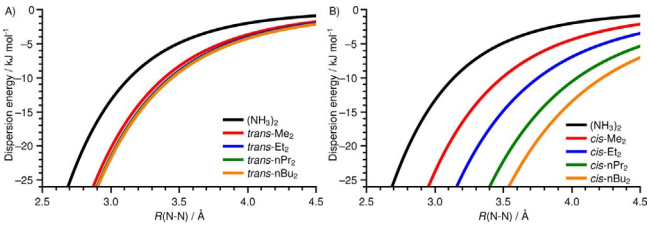

Figure 12. Dispersion contribution of A) *trans* and B) *cis-anti* series.

5.2. Dissociation of Amine Dimers

For *trans* dimers, the difference between rigid and relaxed dissociation will be minimal; it will be larger for *gauche* dimers with large alkyl chains as substituents.

Figure 11 shows the total interaction energies and the dispersionless interaction energies as function of the N–N distance for *trans* and *cis* dimers with *anti* alignment. In the *trans* series, the total interaction energy at the corresponding equilibrium structures increases by 3 kJ mol^{-1} when a hydrogen atom in ammonia is substituted by a methyl group (−12.2 kJ mol^{-1} for $(NH_3)_2$ to −15.4 kJ mol^{-1} for Me_2) and the position of the local minimum decreases from 3.3 Å to 3.2 Å, but further increase of the substituents does not change significantly the stabilization energy and the position of the minimum. The opposite trend is found for the curves of the dispersionless interaction energy, where substitution reduces the stabilization energy by 1.3 kJ mol^{-1} and shifts the minimum of the potential to larger values. Again, further increase of the substituents yields little change in the stabilization energy and the position of the minimum. Both families of energy curves converge rapidly to a limiting curve. Convergence of the curves of the dispersionless and the total interaction energy also implies convergence of the dispersion energy curves; Figure 12 confirms this.

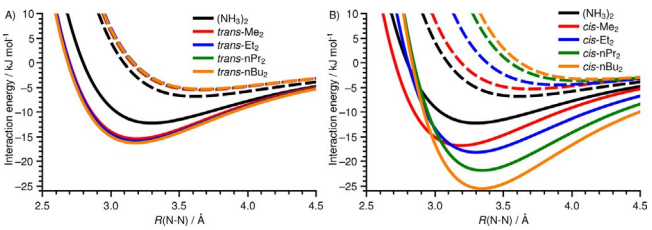

Figure 11. Total interaction energies (solid lines) and dispersionless interaction energies (dashed lines); A) *trans* series, B) *cis-anti* series.

In the *cis-anti* series, there is no convergence in all three families of interaction curves. The total interaction energy increases by 4.6 kJ mol^{-1} when going from the ammonia dimer to the methylamine dimer and the position of the minimum is shifted to 3.2 Å, as in the *trans* series. Further substitutions increase the total interaction energy by 1.4 kJ mol^{-1}, 3.7 kJ mol^{-1}, and 3.6 kJ mol^{-1} and shift the positions of the minima further to larger values (Table 5). There is no evidence for a convergence of the stabilization energies with growing substituents but the minima seem to converge to the distance of the Bu_2 dimer. For the dispersionless interaction energy, we find a monotonic reduction of the well depth and a shift of the distance where the repulsive branch becomes zero to larger values. As expected, there is no convergence of the dispersion energy

Table 5. Total interaction energy E_{Int}, dispersionless interaction energy E_{DL}, dispersion contribution $E_{D_{as}}$ at the equilibrium distances R_{Int}; the * indicates the interaction energies at the minima R_{DL} of the dispersionless energy E_{DL}. Energies in kJ mol^{-1}, distances in Å.

System	R_{Int}	E_{Int}	E_{DL}	$E_{D_{as}}$	R_{DL}	E^*_{DL}	E^*_{Int}
$(NH_3)_2$	3.30	−12.2	−5.0	−7.2	3.62	−6.8	−10.8
trans-Me_2	3.19	−15.4	−1.1	−14.3	3.66	−5.5	−11.9
trans-Et_2	3.19	−15.9	−0.7	−15.3	3.68	−5.4	−12.0
trans-nPr_2	3.18	−16.2	−0.6	−15.7	3.67	−5.4	−12.3
trans-nBu_2	3.18	−16.3	−0.5	−15.8	3.67	−5.4	−12.3
cis-Me_2	3.20	−16.8	−0.1	−16.7	3.69	−5.3	−12.5
cis-anti-Et_2	3.30	−18.2	2.3	−20.5	3.91	−4.5	−12.5
cis-anti-nPr_2	3.35	−21.9	6.4	−28.3	4.06	−3.7	−13.3
cis-anti-nBu_2	3.34	−25.5	9.5	−35.0	4.16	−3.4	−14.2
cis-syn-Et_2	3.25	−17.4	4.5	−21.8	3.92	−3.3	−11.1
cis-syn-nPr_2	3.28	−20.5	8.1	−28.6	4.07	−2.6	−11.4
cis-syn-nBu_2	3.36	−23.3	10.3	−33.6	4.23	−2.3	−11.7
gauche-Et_2	3.27	−19.1	5.2	−24.3	4.04	−3.6	−11.4
gauche-nPr_2	3.29	−21.7	7.3	−29.0	4.15	−3.3	−12.7
gauche-nBu_2	3.29	−23.0	8.2	−31.3	4.12	−3.1	−13.3
iPr_2 I	3.19	−17.9	2.3	−20.2	3.78	−4.4	−12.5
iPr_2 II	3.20	−20.0	4.1	−24.0	3.89	−4.2	−12.8
tBu_2 I	3.25	−20.0	5.3	−25.3	3.99	−3.7	−13.0
tBu_2 II	3.30	−17.9	3.3	−21.2	3.96	−3.8	−12.0

curves either (Figure 12). The interaction energies of the *syn* dimers (see the Supporting Information) are smaller but show the same convergence behavior. Irrespective of the large differences in the shapes of the *trans* and *cis* curves, they both show that the sum of the repulsive exchange repulsion, attractive electrostatic, and induction does not correctly describe the equilibrium distance of the amine complexes and the amount of stabilization. Indeed, at the respective minima of the total interaction energy, the dispersionless interaction energy is close to zero or even positive.

5.3. Energy Components to the Stabilization Energy

The analysis of the stabilization energies in Table 5 at the respective equilibrium distances shows the influence of the size and relative orientation of the substituents on the dimer stability. For all amine dimers with linear substituents, the *trans* structures are least stable. For substituents up to *n*Pr, the *gauche* structures are more stable than the corresponding *cis* structures, for $n\text{Bu}_2$ the order is reversed, and we expect for all larger *n*-alkyl substituents that this trend continues. For $i\text{Pr}_2$, structure II (derived from *cis*-Me_2) is more stable than structure I (derived from *trans*-Me_2), for $t\text{Bu}_2$ it is the other way around. Structures and energies of the dimers with branched substituents are given in the Supporting Information.

The stabilization of *trans*-Me_2 by 3.2 kJ mol^{-1} with respect to the ammonia dimer is caused by a strong increase of dispersion interaction (7.1 kJ mol^{-1}) and a destabilization owing to a moderate decrease (3.2 kJ mol^{-1}) of the attractive dispersionless interaction. Comparison of the energy contributions to the stabilization energies of *trans* and *cis*-Me_2 shows that in the latter the smaller distance between the methyl groups decreases the still stabilizing dispersionless interaction by 1.0 kJ mol^{-1} but increases the stabilization as a result of dispersion interaction by 2.4 kJ mol^{-1}, making *cis*-Me_2 by 1.4 kJ mol^{-1} more stable than *trans*-Me_2. This trend continues in the *cis* series, the increasing destabilization owing to the dispersionless interaction energy is outweighed by the much stronger increase of the stabilizing dispersion interaction. With the growing size of the substituents, the stabilization energy quickly converges to a constant value as do the dispersion contribution and the dispersionless interaction energy. With increasing size of the substituents, the percentage of dispersion interaction gets larger: in the ammonia dimer it is 59%, in Me_2 it is already 93%, and in Bu_2 it is 95% of the stabilization energy. The dispersionless stabilization energy is small but still negative.

In both the *gauche* and the *cis* series, the stabilization energies do not converge but increase monotonically, as do the dispersionless energy and the dispersion energy. In all *cis* dimers, starting with Et_2, the dispersionless interaction energy is positive, thus destabilizing. For the Me_2 dimer, the *anti* and *syn* geometries are identical and moreover, equal to the *gauche* geometry. *Cis* dimers with *syn* alignment have a smaller stabilization energy than the dimers with *anti* alignment; the respective energy differences for Et_2, $n\text{Pr}_2$, and $n\text{Bu}_2$ are 0.8 kJ mol^{-1}, 1.4 kJ mol^{-1}, and 2.2 kJ mol^{-1}. *Anti* structures of small dimers, like Et_2, are more stable because the reduction of the destabilizing dispersionless interaction (2.2 kJ mol^{-1}) is stronger than the reduction of the attractive dispersion interaction (1.3 kJ mol^{-1}); in large dimers, like Bu_2, the dispersionless interaction is reduced by 0.8 kJ mol^{-1} but the attractive dispersion interaction is enlarged by 1.4 kJ mol^{-1} (Table 5). The percentage of the dispersion energy in Me_2 is already 99% and increases to 137% in Bu_2.

By internal rotation in the alkyl groups with respect to C–C single bonds it is possible to create substituents with *clinal* conformations. For the Bu_2 dimer, we created starting geometries for such structures by internal rotations in one substituent, the second was kept in the all-antiperiplanar conformation. Rotation of the propyl group by 90° about the C_α–C_β bond yields the *cis-ab* conformer, rotation of the ethyl group by 90° about the C_β–C_γ bond yields the *cis-bc* conformer. The optimized geometries are shown in Figure 13; the stabilization energies are −25.5 kJ mol^{-1} and −22.7 kJ mol^{-1}, respectively.

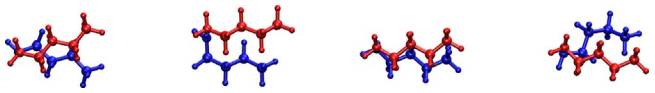

Figure 13. *Cis* dimers of Bu_2. From left to right: *cis-anti*, *cis-ab*, *cis-syn*, *cis-bc*.

Small *gauche* dimers like Et_2 are more stable than the corresponding *cis* dimers, but for the larger substituents the trend changes and the *cis* isomers are more stable. For these dimers, the high flexibility of the alkyl chains allows that the terminal parts of the substituents come in close contact without significant stretching of the central moiety. This is not possible with small substituents, for example, ethyl groups.

The four optimized *cis* and the *gauche* structures have stabilization energies lying in an energy interval of 2.8 kJ mol^{-1}. If we make rotations about single bonds not only in one but in both substituents, we expect some more dimer structures with similar energies. With increasing length of the substituents, the number of different equilibrium structures with similar stabilization energies will strongly increase.

Also for dimers with branched substituents, we get structures with similar energies. Both stable structures for the $i\text{Pr}_2$ and $t\text{Bu}_2$ dimers have energies that differ by 2.1 kJ mol^{-1}. Although both the repulsive dispersionless interaction energy and attractive dispersion energy are larger in the more stable dimers, it is the much larger attractive component that is responsible for the strong stabilization.

That the balance of attractive dispersion interaction and repulsive dispersionless interaction is responsible for the dimer structures can be demonstrated by analyzing the *zigzag* structures, which were found only with dlDF + D_{as} (Table S8 in the Supporting Information). In *zigzag*-Me_2, each methyl group is not only near to the nitrogen atom it is bonded to, it is also much closer to the other nitrogen atom than it is in *trans*-Me_2. Owing to a strong increase of exchange repulsion, the dispersionless energy increases by 2.3 kJ mol^{-1}, making the dispersionless energy positive, thus destabilizing. However, the attractive dispersion interaction is larger than in *trans*-Me_2 by

3.1 kJ mol^{-1}, so that the sum of both contributions makes *zigzag*-Me_2 more stable by 0.8 kJ mol^{-1} than *trans*-Me_2. In *zigzag*-Et_2, the terminal methyl groups are still rather close to the central moiety, causing both an increase of dispersion interaction and dispersionless interaction and, concomitantly, making *zigzag*-Et_2 more stable than *zigzag*-Me_2 by 1.2 kJ mol^{-1}; *zigzag*-Pr_2 dimer is more stable by 1.1 kJ mol^{-1} than *zigzag*-Et_2 and *zigzag*-Bu_2 is more stable than *zigzag*-Pr_2 by 0.4 kJ mol^{-1}. We expect that convergence is reached for dimers with pentyl or hexyl substituents.

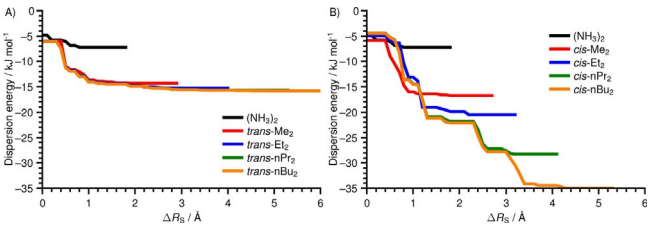

Figure 14. The cumulative increase of the dispersion contribution to dimer stability as a function of the increase ΔR_S A) in the *trans*, and B)in the *cis* series.

5.4. Origin of Dimer Stabilization

The stabilization energies converge in the *trans* series to the value for Pr_2, but in the *cis* and the *gauche* series the stabilization energies seem to grow constantly by a finite increment, which is about 3 kJ mol^{-1} per CH_2 group for *cis* dimers with *syn* alignment, about 4 kJ mol^{-1} per CH_2 group for *cis* dimers with *anti* alignment, and 1.5 kJ mol^{-1} per CH_2 group for *gauche* dimers. These constant increases of the stabilization energies are always due to a large increase in the stabilizing dispersion interaction and a smaller increase in the destabilizing dispersionless interaction. The latter is itself the sum of a large increment in the destabilizing exchange repulsion and a smaller increment in attractive electrostatics and induction. Although the individual interactions have different range, their sum is nevertheless short-ranged, and therefore each additional methylene group sees only the nearest atoms in the opposite alkyl chain. In the study of non-covalent interactions between carbon nanotubes and aromatic adsorbates, we called the set of all intermolecular atom pairs "seeing each other" the "contact zone" of the non-covalent interaction[41–43] and we showed that only atoms in the contact zone contribute to the interaction energy. The size of the contact zone is proportional to the intersection of the contact surfaces of the interacting molecules, as defined by Richards.[44] The intersection of contact surfaces is especially helpful for explaining the strong interaction between several parallel aligned alkyl chains and the much smaller interaction between globular alkyl groups, but it is not so helpful for analyzing the difference in interaction between *cis* and *trans* dimers. To do this, we calculated the interaction energy of the intermolecular atom pairs lying inside a sphere with the midpoint in the center of the central moiety and studied the increase in the interaction by gradually increasing the radius of the sphere, R_S. This method was also used in our study of the dispersion interaction between the substituents in alcohol dimers.[23] In Figure 14, we show the dispersion interaction $E_{D_{as}}$ for different dimers as a function of the increase ΔR_S of R_S, the zero of ΔR_S corresponds to R_S being half of the respective N···N equilibrium distances, that is, half of the R_{Int} values from Table 5. In the ammonia dimer, the major contribution comes from the atoms of the N–H···N central moiety, with increasing R_S the sphere contains the remaining five hydrogen atoms; increasing the radius by $\Delta R_S \approx 0.35$ Å, one additional hydrogen atom is inside the sphere, when R_S is approximately 2.5 Å, corresponding to $\Delta R_S \approx 0.9$ Å, also the remaining four hydrogen atoms lie inside the sphere. The first contributions to the interaction energy for *trans*-Me_2 come again from the atom pairs of the central moiety lying within the sphere with $R_S = 1.6$ Å, increase of R_S by $\Delta R_S \approx 0.4$ Å includes the carbon atoms of the methyl groups and therefore gives a large contribution to the interaction energy, all contributing intermolecular atom pairs lie within a sphere with $R_S = 2.5$ Å (or $\Delta R_S = 0.9$ Å) and further enlargement of R_S does not change $E_{D_{as}}$ anymore. The $E_{D_{as}}$ curve for *trans*-Et_2 looks very similar to the Me_2 curve, which means that only the α-CH_2 groups make substantial contributions to the interaction energy; this assumption is corroborated by the shape of the Pr_2 and Bu_2 curves, which are essentially identical to the Et_2 curve, as well as by the left subfigure of Figure 15, showing that CH_2 groups that are more distant than the diameter of the second sphere do not contribute to the stabilization.

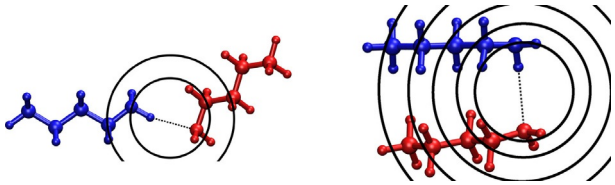

Figure 15. Spheres enclosing parts of *n*Bu_2. The centers are the midpoint of the N–N distance, the radii R_S correspond to the positions of the jumps in the energy curve in Figure 14. Left for the *trans*, and right for the *cis* dimer.

The curves for the *cis* dimers look very different. The Me_2 curve becomes constant for $\Delta R_S \approx 0.9$ Å as in the *trans* series, the magnitude of $E_{D_{as}}$ is slightly larger, because in the *cis* dimer the methyl groups not only see the atoms of the central moiety but also each other. When going from Me_2 to Et_2, the distance of the terminal methyl group increases as in the *trans* series but now each methyl group not only "sees" the other methyl group, but also the neighboring CH_2 group. The Bu_2 curve shows nicely how the three CH_2 and the terminal CH_3 group contribute to $E_{D_{as}}$: the first contribution from the substituents stems from the α-CH_2 groups, which see the atoms of the central moiety as well as each other. The contributions of the β, γ, etc., groups are smaller than those of the α groups because each new CH_2 group sees only the opposite methyl and the neighboring CH_2 group but not the electron-rich atoms of the central moiety, however, these contributions are rather constant.

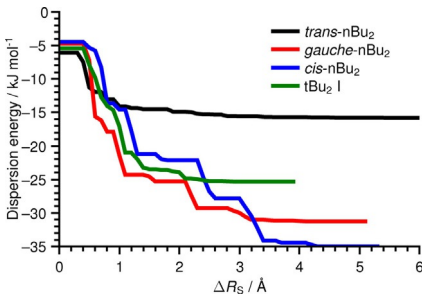

Figure 16. The cumulative increase of the dispersion contribution to the stability of four Bu_2 dimers as a function of ΔR_S.

The equilibrium structures of *gauche* dimers with small substituents are different from both the *trans* and *cis* dimers (Figure 16); when the substituents increase the parts of the alkyl groups next to the central moiety are more distant than in a *cis* dimer but the more distant parts will adopt a parallel structure as in the *cis* series. In *gauche* Bu_2, the first contributions are smaller than in the *cis* dimer but the more distant parts of the butyl groups give similar contributions as for the *cis* dimer. For branched, bulky substituents, the development of the $E_{D_{as}}$ curves is in between the corresponding *trans* and *cis* curves (Figure 16). Amine dimers with bulky substituents are always *trans*-like, which means the bulky substituents are as far away from each other as possible. The growth of tBu_2 in the spherical shells shows first the contribution of the two α carbon atoms, which is smaller than that of two CH_2 groups in *trans*-Bu_2, and then the contributions of six methyl groups. Their contribution is larger than that of the two β-CH_2 groups, but smaller than the contribution of the four β- and γ-CH_2 groups in *cis*-Bu_2. The different dispersion contributions determine the ordering of both the dispersionless and the total interaction energy curves, as shown in Figure 17) for the Bu_2 dimers.

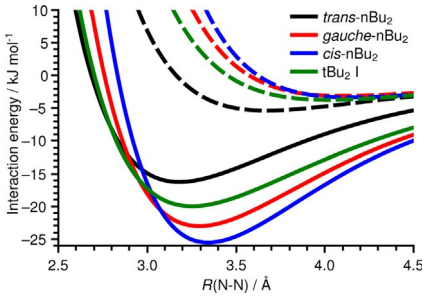

Figure 17. Total interaction energies (full lines) and dispersionless interaction energy (dashed lines) of different Bu isomers.

6. Discussion

Our study does not support the assumption that amine dimers are solely stabilized by hydrogen bonds. The structure of the central moiety does not dramatically change when going from the eclipsed ammonia dimer to the amine dimers, but the stabilization energy increases considerably and, moreover, also depends on the size and position of the alkyl groups. This is incomprehensible if one believes that the atoms of the central moiety are responsible for hydrogen bonding. If one believes that dispersion is less important than electrostatics for hydrogen bonding, it is hard to explain why the dispersionless stabilization energy is only a fraction of the total stabilization energy, and why the local minima of the dispersionless interaction energy are at much larger distances than the minima of the total interaction energy, and why correct stabilization energies are only obtained when dispersion interaction is accounted for.

Figure 18 shows the energy contributions to the dispersionless interaction energy for the water dimer as obtained from our SAPT study[23] together with the dispersionless interaction energy of the ammonia dimer, calculated with dIDF. Both dispersionless interaction energy curves have extremely shallow potential wells and a zero at about 85% of the positions of the respective minima. As the curves for the water dimer show, the dispersionless interaction energy at large distances is dominated by electrostatics and induction because exchange has already died away there; at short distances exchange dominates the dispersionless interaction energy. The slope at zero is the sum of the large positive slope of the attractive interaction and of the large negative slope of the repulsive exchange, it is, in magnitude, much smaller than either of the contributions. As the depths of the potential wells show, the contribution of electrostatics and induction in the ammonia dimer is much smaller than in the water dimer; the smaller slope for the ammonia dimer suggests that also the repulsive exchange is smaller in the ammonia dimer. Adding the dispersion contribution to the dispersionless interaction energy roughly doubles the well depths for both dimers, but as the dispersion contribution for the ammonia dimer is also smaller in magnitude, the stabilization energy for the ammonia dimer is still about half the stabilization energy for the water dimer (Figure 19). Adding the dispersion interaction shifts the minima of the total interaction energies to distances that are about 10% smaller than the minima of the dispersionless interaction energy curves, and also the zeros of the total interaction ener-

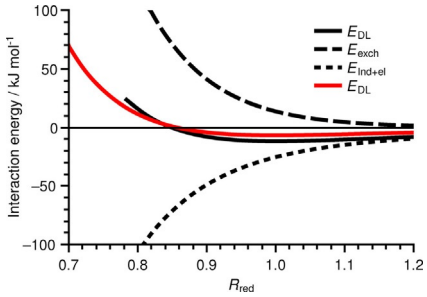

Figure 18. Black curves: SAPT energies (dispersionless, exchange, and induction + exchange) of the water dimer. Red curve: dIDF energy of the ammonia dimer. The abscissa is the reduced inter-monomer distance $R_{red} = R/R_{min}$ at the minimum of the dispersionless energy curve.

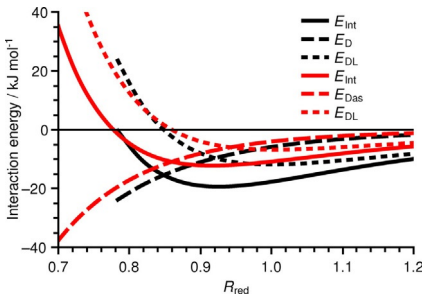

Figure 19. Total interaction, dispersion, and dispersionless energies. Black curves: SAPT energies of the water dimer. Red curves: dIDF + D_{as} energies of the ammonia dimer. The abscissa is the reduced inter-monomer distance $R_{red} = R/R_{min}$ at the minimum of the dispersionless energy curve.

gies are shifted to smaller distances. Without consideration of dispersion interactions, both dimers are more floppy and more unstable.

The qualitative agreement of the interaction energy curves for both dimers is striking and shows that 1) the assumption that the dominating attractive interaction is electrostatics is not true, dispersion interaction is at least as important and 2) representing exchange repulsion in a hydrogen-bonded complex by a hard sphere potential is completely at odds with the shapes of both the dispersionless and total interaction energies. As dispersion depends on the polarizability of the interacting molecules and the polarizabilities of water and ammonia are determined by the heavy element atoms, that is, oxygen and nitrogen, we assume that these findings also hold for amine dimers and alcohol dimers. For dimers with atoms from periods higher than 2 this has to be proven.

Dispersion interaction is crucial for the molecular structure of non-polar molecules. Non-branched alkane molecules with up to 17 or 18 carbon atoms prefer an extended structure with the all-antiperiplanar conformation being most stable; larger molecules can adopt a hairpin structure but need at least four *gauche* dihedral angles to bring linear chain segments into contact.[45] The costs for these rotations are outweighed by the energy gain resulting from the interaction between the chain segments. In amine dimers, but also in alcohol dimers, the central moiety allows the hairpin structure in *cis* dimers without any additional costs for internal rotations, the *trans* conformer is not the most stable but the least stable conformer.

Condensed matter properties, like the boiling point, represent the strength of intermolecular interaction in the condensed phase. For water and ammonia, the boiling points are very different with +100 °C and −33 °C, respectively, for methanol and methylamine the difference between the boiling points of +65 °C and −6 °C, respectively, is already smaller, but for the *n*-decyl-substituted species they are very similar, +231 °C and +221 °C, respectively. In both series, alcohols and amines, we observe a monotonic increase of the boiling point with increasing length of the alkyl groups,[46] which demonstrates the increasing importance of the interaction between the substituents. After all, the atomic percent of the alkyl groups in butylamine is already 81 %.

Comparison of the boiling points of all butyl-amines and butyl-alcohols shows the influence of the shape of the substituents: the boiling points for *n*-butylamine, *iso*-butylamine, *sec*-butylamine, and *tert*-butylamine are 79 °C, 66 °C, 63 °C, and 45 °C, respectively; the boiling points for the corresponding butyl-alcohols are 118 °C, 108 °C, 99 °C, and 83 °C, respectively.[47] In both series, the species with the linear *n*-butyl substituents have the highest and the species with the globular *tert*-butyl substituents have the lowest boiling points. The contact surfaces of *n*-alkyl chains can be regarded as tubes, whereas those of globular alkyl groups are roughly spheres. Accordingly, the contact zone for parallel aligned tubes is always much larger than that for spheres in close contact, the stronger interaction between the *n*-alkyl groups explains the higher values of the boiling points.

Stressing the role of dispersion interaction between large substituents does not mean that the polar groups forming the central moiety are unimportant; this would be completely wrong as, for example, the increase of the respective boiling points with increasing number of amino groups shows: the respective values for propylamine, 1,3-propanediamine, and 1,2,3-propanetriamine are 49 °C,[47] 139 °C,[47] and 190 °C[48]. But the boiling points of 116 °C, 139 °C, 158 °C, 179 °C, and 204 °C for the series 1,2-diaminoethane, propane-1,3-diamine, butane-1,4-diamine, pentane-1,5-diamine, and hexane-1,6-diamine,[47] show again that the boiling point also increases when the non-polar part of the molecule increases. The result of our investigations of the interactions between the substituents in dimers can be used to explain the interactions between dimers as well; the interaction between linear alkyl groups is the same irrespective of whether they belong to a single dimer or to different dimers. The short-range attractive interactions become operative as soon as the two alkyl chains are brought into close contact. In amines or alcohols, this is done by the central moiety; terminal polar groups in diamines or dioles will further reduce the distance between the alkyl chains and, thus, increase the attractive interaction between the substituents. The boiling point of 1-propanol with four heavy atoms and one polar OH group (97 °C)[47] is nearly identical with the 98 °C of heptane[47] with seven heavy atoms but no polar group. This means that there are strong attractive interactions between long alkyl chains even without polar groups forming hydrogen bonds, but hydrogen bridges enhance the attraction considerably. An analogy of the attraction between alkyl chains that are connected by hydrogen bonds is reinforced concrete: ubiquitous dispersion is the concrete and the hydrogen bridges are the rebars. Claiming that the bonding between polyalcohols or polyamines is only due to the hydrogen bridges, means ignoring the concrete and considering only the rebars. Stressing only the role of dispersion interaction would mean ignoring the rebars and considering only the concrete.

Internal rotation in long alkyl chains gives rise to a large number of rotamers; when several of them are parallel aligned this gives rise to a large number of equilibrium structures with similar stabilization energies. The high energetic degeneracy of such structures, which are absent in the gas phase, are the origin of the entropy term in the free energy, which is necessa-

ry to understand hydrophobic interactions. The statement by Wolfenden and Lewis[17] "that a strong favorable interaction among alkane molecules in liquid alkanes gives a strong favorable transfer energy for passage of an alkane from vapor into liquid alkane" does not do justice to this phenomenon because it emphasizes only the energy contribution to the transfer free energy. The conformational entropy contribution must not be ignored.

If the atomic group connecting the substituents in a *cis* dimer is replaced by say an ether oxygen no one would say that the stability of the hairpin structure is caused by covalent bonding between the substituents and the bridging oxygen atom. Indeed, the stability of such structures has to be attributed to the intramolecular dispersion interaction,[22] which is crucial for the understanding of the geometry of large molecular systems, as mentioned by Wagner and Schreiner.[13]

7. Conclusions

The role of dispersion interactions in hydrogen-bonded complexes is underrated and the role of electrostatics is grossly overstated. We showed that in amine dimers, the attractive interaction between the alkyl substituents is dominated by dispersion interactions, which depend on the size, the shape, and the relative orientation of the substituents. Dimers of small amines are described as stable even without dispersion interactions, although the stabilization energy is too small and the equilibrium structure is not correct, but dimers of amines with large substituents in close contact are not stable unless dispersion interactions between the substituents are accounted for. Cluster of amines or amine dimers have a large number of energetically similar equilibrium structures because of the many conformers each of the alkyl groups can have. The degeneracy of these structures is the origin of a conformational entropy contribution. The energetic part of hydrophobic interactions in liquid alkanes or amines with large alkyl substituents is dominated by dispersion interactions, the entropic part has its origin in the high degeneracy of clusters of molecules.

Acknowledgments

Helpful discussions with Krzysztof Szalewicz and Bogumil Jeziorski are gratefully acknowledged. The authors acknowledge financial support by the University of Graz.

Conflict of Interest

The authors declare no conflict of interest.

Keywords: amine dimers · density functional theory · dispersion interactions · electrostatic interactions · hydrogen bonds

[1] S. J. Cole, K. Szalewicz, G. D. Purvis, R. J. Bartlett, *J. Chem. Phys.* **1986**, *84*, 6833 – 6836.
[2] K. Szalewicz, S. J. Cole, G. D. Purvis, W. Kolos, R. J. Bartlett, *J. Chem. Phys.* **1988**, *89*, 3662 – 3673.
[3] S. Rybak, B. Jeziorski, K. Szalewicz, *J. Chem. Phys.* **1991**, *95*, 6576 – 6601.
[4] S. Ryback, K. Szalewicz, B. Jeziorski, G. Corongiu, *Chem. Phys. Lett.* **1992**, *199*, 567 – 573.
[5] V. F. Lotrich, H. L. Williams, K. Szalewicz, B. Jeziorski, R. Moszynski, P. E. S. Wormer, A. van der Avoird, *J. Chem. Phys.* **1995**, *103*, 6076 – 6092.
[6] R. Rohs, S. West, A. Sosinsky, P. Liu, R. Mann, B. Honig, *Nature* **2009**, *461*, 1248 – 1253.
[7] M. Ahmad, W. Gu, T. Geyer, V. Helms, *Nat. Commun.* **2011**, *2*, 261.
[8] J. Guo, X. Meng, J. Chen, J. Peng, J. Sheng, X.-Z. Li, L. Xu, J.-R. Shi, E. Wang, Y. Jiang, *Nat. Mater.* **2014**, *13*, 184 – 189.
[9] G. A. Jeffrey, *An Introduction to Hydrogen Bonding*, Oxford University Press, New York, NY, **1997**.
[10] G. R. Desiraju, T. Steiner, *The Weak Hydrogen Bond*, Oxford University Press, New York, NY, **2001**.
[11] S. J. Grabowski, *Hydrogen Bonding—New Insights*, Springer, Dortrecht, **2006**.
[12] G. Gilli, P. Gilli, *The Nature of the Hydrogen Bond*, Oxford University Press, New York, NY, **2009**.
[13] J. P. Wagner, P. R. Schreiner, *Angew. Chem. Int. Ed.* **2015**, *54*, 12274 – 12296; *Angew. Chem.* **2015**, *127*, 12446 – 12471.
[14] R. L. Baldwin, *FEBS Lett.* **2013**, *587*, 1062 – 1066.
[15] W. Kauzmann, *Adv. Protein Chem.* **1959**, *14*, 1 – 63.
[16] R. L. Baldwin in *Protein Folding Handbook, Part I* (Eds.: J. Buchner, T. Fiefhaber), Wiley-VCH, Weinheim, **2014**.
[17] R. Wolfenden, C. A. A Lewis Jr., *J. Theor. Biol.* **1976**, *59*, 235 – 321.
[18] I. G. Kaplan, *Intermolecular Interactions: Physical Picture, Computational Methods and Model Potentials*, John Wiley and Sons, Chichester, **2006**.
[19] A. Stone, *The Theory of Intermolecular Forces, 2nd ed.*, Oxford University Press, Oxford, **2013**.
[20] A. Salam, *Non-Relativistic QED Theory of the van der Waals Dispersion Interaction*, Springer, Cham, Switzerland, **2016**.
[21] S. Grimme, *Comput. Mol. Sci.* **2011**, *1*, 211 – 228.
[22] S. Grimme, A. Hansen, J. G. Brandenburg, C. Bannwarth, *Chem. Rev.* **2016**, *116*, 5105 – 5154.
[23] J. Hoja, A. F. Sax, K. Szalewicz, *Chem. Eur. J.* **2014**, *20*, 2292 – 2300.
[24] K. Pernal, R. Podeszwa, K. Patkowski, K. Szalewicz, *Phys. Rev. Lett.* **2009**, *103*, 263201.
[25] A. J. Misquitta, R. Podeszwa, B. Jeziorski, K. Szalewicz, *J. Chem. Phys.* **2005**, *123*, 214103.
[26] A. Hesselmann, G. Jansen, M. Schütz, *J. Chem. Phys.* **2005**, *122*, 014103.
[27] R. Podeszwa, K. Pernal, K. Patkowski, K. Szalewicz, *J. Phys. Chem. Lett.* **2010**, *1*, 550 – 555.
[28] A. D. Becke, *J. Chem. Phys.* **1993**, *98*, 5648 – 5652.
[29] S. Grimme, *J. Comput. Chem.* **2006**, *27*, 1787 – 1799.
[30] S. Grimme, J. Antony, S. Ehrlich, H. Krieg, *J. Chem. Phys.* **2010**, *132*, 154104.
[31] J. Rezác, P. Jurecka, K. Riley, J. Cerný, H. Valdes, K. Pluháckova, K. Berka, T. Rezác, M. Pitonák, J. Vondrášek, P. Hobza, *Collect. Czech. Chem. Commun.* **2008**, *73*, 1261 – 1270.
[32] T. Dunning Jr., *J. Chem. Phys.* **1989**, *90*, 1007 – 1023.
[33] R. Kendall, T. Dunning Jr., R. Harrison, *J. Chem. Phys.* **1992**, *96*, 6796 – 6806.
[34] D. Woon, T. Dunning Jr., *J. Chem. Phys.* **1993**, *98*, 1358 – 1371.
[35] D. Woon, T. Dunning Jr., *J. Chem. Phys.* **1994**, *100*, 2975 – 2988.
[36] S. Boys, F. Bernardi, *Mol. Phys.* **1970**, *19*, 553 – 566.
[37] M. Valiev, E. Bylaska, N. Govind, K. Kowalski, T. Straatsma, H. V. Dam, D. Wang, J. Nieplocha, E. Apra, T. Windus, W. de Jong, *Comput. Phys. Commun.* **2010**, *181*, 1477 – 1489.
[38] M. D. Hanwell, D. E. Curtis, D. C. Lonie, T. Vandermeersch, E. Zurek, G. R. Hutchison, *J. Cheminf.* **2012**, *4*, 17.
[39] L. Gráfová, M. Pitonák, J. Rezác, P. Hobza, *J. Chem. Theory Comput.* **2010**, *6*, 2365 – 2376.
[40] J. Rezác, K. E. Riley, P. Hobza, *J. Chem. Theory Comput.* **2011**, *7*, 2427 – 2438.
[41] R. J. Maurer, A. F. Sax, *Phys. Chem. Chem. Phys.* **2010**, *12*, 9893 – 9899.
[42] S. Glanzer, A. F. Sax, *Mol. Phys.* **2013**, *111*, 2427 – 2438.
[43] C. Lechner, A. F. Sax, *Appl. Surf. Sci.* **2017**, *420*, 606 – 617.
[44] F. M. Richards, *Ann. Rev. Biophys. Bioengineering* **1977**, *6*, 151 – 176.

[45] N. O. B. Lüttschwager, T. N. Wassermann, R. A. Mata, M. A. Suhm, *Angew. Chem. Int. Ed.* **2013**, *52*, 463 – 466; *Angew. Chem.* **2013**, *125*, 482 – 485.
[46] W. M. E. Haynes, *CRC Handbook of Chemistry and Physics*, 94th Ed., CRC Press, Boca Raton, FL, **2013**.
[47] GESTIS-Stoffdatenbank, http://www.dguv.de/ifa/gestis/gestis-stoffdatenbank/index.jsp, accessed 21 November, 2016.
[48] ChemSpider, http://www.chemspider.com/, accessed 21 November, 2016.

Received: March 10, 2017
Version of record online June 27, 2017

